Journal of Hazardous Materials 191 (2011) 240–248

Contents lists available at ScienceDirect

Journal of Hazardous Materials

journal homepage: www.elsevier.com/locate/jhazmat

Sorption characteristics of fluoride on to magnesium oxide-rich phases calcined at different temperatures

Keiko Sasaki*, Naoyuki Fukumoto, Sayo Moriyama, Tsuyoshi Hirajima

Department of Earth Resources Engineering, Kyushu University, Fukuoka 819-0395, Japan

ARTICLE INFO

Article history:
Received 1 February 2011
Received in revised form 8 April 2011
Accepted 16 April 2011
Available online 22 April 2011

Keywords:
Magnesium oxides
Fluoride
Calcinations
Sorption isotherm
Temperature programmed desorption of CO_2

ABSTRACT

The effect of calcination temperature during production of magnesium oxide-rich phases from $MgCO_3$ on the sorption of F^- ions in the aqueous phase has been investigated. Magnesium oxide-rich phases were formed by calcination at over 873 K for 1 h. Higher calcination temperatures produced more crystalline MgO with smaller specific surface area and provided larger values of the total basicity per unit surface area. The higher calcination temperatures lead to slower F^- removal rate, and lower equilibrium F^- concentrations, when the equilibrium F^- concentrations are less than 1 mmol dm^{-3}. Larger total basicity per unit surface area made the reactivity with F^- ions in aqueous phase more feasible, resulting in a greater degree of F^- sorption. For equilibrium F^- concentrations more than 1 mmol dm^{-3}, lower calcination temperatures favored the co-precipitation of F^- with $Mg(OH)_2$, probably leading to the formation of $Mg(OH)_{2-x}F_x$, and the achievement of larger sorption density. This is the first paper which describes the relationship between the solid base characteristics obtained by CO_2-TPD for MgO with different calcination temperatures as a function of the reactivity of F^- sorption in the aqueous phase.

© 2011 Elsevier B.V. All rights reserved.

1. Introduction

Fluorine (F) is known as an essential element for animal mineralization of bones and the formation of dental enamel. However, excess intake leads to physical disorders such as dental fluorosis, stiffened and brittle bones and joints, deformation of knee and hip bones and finally paralysis, making the person unable to walk or stand [1,2].

Due to natural causes and/or anthropologic activities such as intensively cultivated fields [3], the disposal of hazardous waters, mining drainages, semi-conductor and glass industry drainages and solid waters, sewage disposal and surface impoundments [4], the contamination of groundwater with fluoride (F^-) has become clear, gradually leading to serious problems. The maximum contamination limits (MCLs) of F^- ions are regulated to be less than 1 mg L^{-1} for drinking water and 10 mg L^{-1} for industrial discharges by the WHO [5]. In Japan the MCLs for F^- were established in 1998 to be 0.8 mg L^{-1} and 8.0 mg L^{-1} for drinking water and industrial discharges, respectively [6]. The MCL values are not completely consistent among the US, EU and Japan. This means that the regulation of F^- ions is subtly influenced by protection of industrial activities as well as the protection of human health and ecology in each country. The toxicity of F^- ions to humans is not yet fully understood.

The conventional treatment for F^- is precipitation of CaF_2 by the addition of lime followed by coagulation with alumina. Permeable reactive barriers (PRBs) have been developed as in situ groundwater remediation for the removal of a variety of contaminants [7,8]. However, PRBs have not yet been used officially to remove F^- and H_3BO_3 in groundwater, because cost-effective reactive materials are yet to be found. The authors have recently reported the performance of a PRB column including MgO for the removal of H_3BO_3 [9].

Several sorbents have been previously investigated to discover effective defluorinating agents with reasonable cost: geomaterials such as activated alumina [10], activated carbon [11], lime [12], magnesium–aluminium oxide [13,14], serpentine [15], layered double hydroxides (LDHs) [16–18], metallic oxide mixtures of industrial wastes from Al manufacturing, which consist of 40% quartz and 9% kaolin and trace amounts of metallic oxide and sulfates [19], brick powder [20], hydrated cement [21], geomaterials from mining industries in which hematite and goethite are included as major components [22] and attapulgite [23], which is a hydrated magnesium aluminium silicate present in nature as a fibrous clay mineral containing ribbons of a 2:1 structure. LDHs might be promising materials as sorbents for anionic species, but they are naturally less abundant.

In the present study, MgO produced by the calcination of magnesite ($MgCO_3$), a natural mineral, at different temperatures is

* Corresponding author. Tel.: +81 92 802 3338; fax: +81 92 802 3338.
E-mail address: keikos@mine.kyushu-u.ac.jp (K. Sasaki).

0304-3894/$ – see front matter © 2011 Elsevier B.V. All rights reserved.
doi:10.1016/j.jhazmat.2011.04.071

investigated as a simple model of sorbents for F^-, because of its high reactivity, wide availability and its high potential for development into more complicated sorbents, such as multi-metallic oxides. The relationship between the calcination temperatures of MgO with F^- sorption density will be discussed, along with a possible mechanism.

2. Experimental

$MgCO_3$ reagent (special grade, Sigma–Aldrich, St. Louis, MO, US) was calcined to produce MgO-rich phases by heating at 873 K, 1037 K, 1273 K and 1373 K for 1 h. The products are named as 873-MgO, 1037-MgO, 1273-MgO and 1373-MgO, respectively, and were stored in a vacuum dessicator until use. They were characterized by X-ray diffraction with CuKα, 40 kV, 20 mA (XRD, Multi Flex, Rigaku, Akishima, Japan), scanning electron microscopy (SEM, VE-9800, KEYENCE, Osaka, Japan) with 15 kV of accelerating voltage, transmission electron microscopy (TEM, JEM-200CX, JEM-2000FX, JEOL, Tokyo, Japan), measurement of the specific surface area using the seven-point N_2-adsorption BET method (AUTOSORB-1, YUASA, Osaka, Japan), and temperature programmed desorption curves (TPD, BELCAT-B, BEL JAPAN Inc., Toyonaka, Japan), using CO_2 as a probe gas. The CO_2-TPD curves were measured with a temperature ramp rate of 3.3 °C/min after degassing by heating the samples at 500 °C, and analyzed using BELCAT Chem Master software Ver. 2.3.9 (BEL JAPAN Inc., Toyonaka, Japan) to evaluate the basicity and the number of base sites of the calcined products, mainly consisting of MgO.

The sorption of F^- ions on to the products calcined at different temperatures was investigated at 298 K. 0.61–54.76 mmol dm^{-3} F^- solutions were prepared using NaF (special grade, Wako, Osaka, Japan) at pH 6.41 ± 0.45. For the sorption experiments, 0.100 g of calcined MgO-rich phase sorbents was added to 40 cm^3 of the F^- solutions, followed by shaking at 100 rpm and 25 °C. In some batch experiments, calcined MgO-rich phase sorbents were replaced with $MgCO_3$ reagent.

In preliminary experiments, it was confirmed that the sorption equilibrium is achieved within 120 h under the conditions used. After sorption equilibrium, 4 cm^3 of supernatant was taken out and filtered by 0.45 μm pore size membrane filters for determination of F^- concentrations by ion chromatography (DIONEX ICS-90, Osaka, Japan) and Mg^{2+} concentrations by atomic absorption spectrometry (SOLAAR-AAS, Thermo, Yokohama, Japan). Solid residues were collected by filtration using a pore size of 0.45 μm and the final solution pH was measured by a pH meter (HM-30G DKK-TOA, Tokyo, Japan). Solid residues after sorption were also characterized by XRD and SEM in the same manner as for the sorbents before sorption.

3. Results and discussion

Fig. 1 shows the XRD patterns of the calcined $MgCO_3$ at 873–1373 K. A single phase of MgO (JCPDS 45-946) was observed in the XRD patterns for 1373 K-MgO and 1273 K-MgO, while additional phases are observed along with MgO in the calcined products at below 1073 K. These peaks were assigned to uncalcined basic magnesium carbonates (JCPDS 35-454, 35-680), indicating that complete decarbonation was not always achieved by calcination at below 1073 K. It is natural that the peaks assigned to MgO became weaker and much broader with decrease in calcination temperature. XRD intensities assigned to MgO clearly increased with increase in calcination temperatures, and are reflected by not only the contents of MgO but also crystallinity of MgO. More than 1273 K in calcination temperature no secondary phases were observed by XRD.

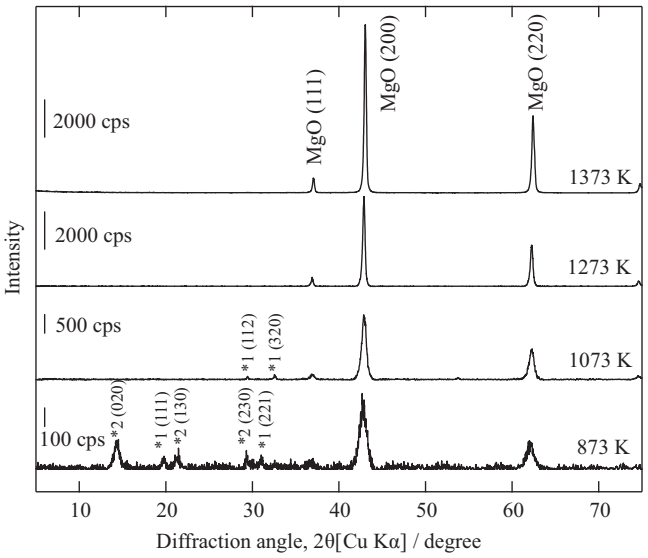

Fig. 1. XRD patterns of products after calcination of $MgCO_3$ at different temperatures for 1 h at (a) 873 K, (b) 1073 K, (c) 1273 K, and (d) 1373 K. (*1) $Mg_2CO_3(OH)_2{\cdot}0.5H_2O$ (JCPDS 37-454), (*2) $MgCO_3{\cdot}5H_2O$ (JCPDS 35-680).

Fig. 2 shows SEM images for the calcined products. The morphologies of these products are similar to each other and independent of the calcination temperature, appearing as rods 50–60 μm by 5–6 μm. However, the specific surface area was dependent on the calcination temperature: 50 $m^2\,g^{-1}$ for 873 K-MgO, 79 $m^2\,g^{-1}$ for 1073 K-MgO, 29 $m^2\,g^{-1}$ for 1273 K-MgO, and 13 $m^2\,g^{-1}$ for 1373 K-MgO. Except for 873 K-MgO, the specific surface area decreased with the calcination temperatures. This suggests that there are structural differences in the nano-domains between the products calcined at different temperatures.

TEM images for the calcined products are shown in Fig. 3. Larger crystal sizes can be observed at higher calcination temperatures. Electron diffraction patterns confirmed that higher calcination temperature led to higher crystallinity. It is shown that there is a difference in crystal size of MgO between 1273 K and 1373 K in calcination temperature, and that there is no amorphous phase in both samples. This indicates that increase in XRD peak intensities assigned to MgO with increase in calcination temperature from 1273 K to 1373 K (Fig. 1) attributes to mainly increase in crystallinity as MgO. Thus, the TEM observations clearly demonstrated the effect of the calcination temperature on the nano-characterization of the calcined magnesium oxide products.

It is known that magnesium oxide is a strong solid base and there are optimal pretreatment temperatures for different chemical reactions [24]. This arises from the fact that there are several base sites with different basicities observed in the CO_2-TPD curves for MgO [25]. The CO_2-TPD curves for the calcined products at 1073 K, 1273 K and 1373 K were collected in the CO_2-desorption temperature range from 300 K to 700 K as shown in Fig. 4. They can be separated into three components with different basicities in the calcination products, including mainly MgO. Analysis of the peak positions, peak areas, and the corresponding sorbed CO_2 quantities are summarized in Table 1. The total intensity per unit surface area was greater in the order 1373 K-MgO, 1273 K-MgO and 1073 K-MgO. The peak positions of the CO_2-TPD curves for MgO are in good agreement with a previous report by Fan et al. [26]. Interestingly, the proportion of the dif-

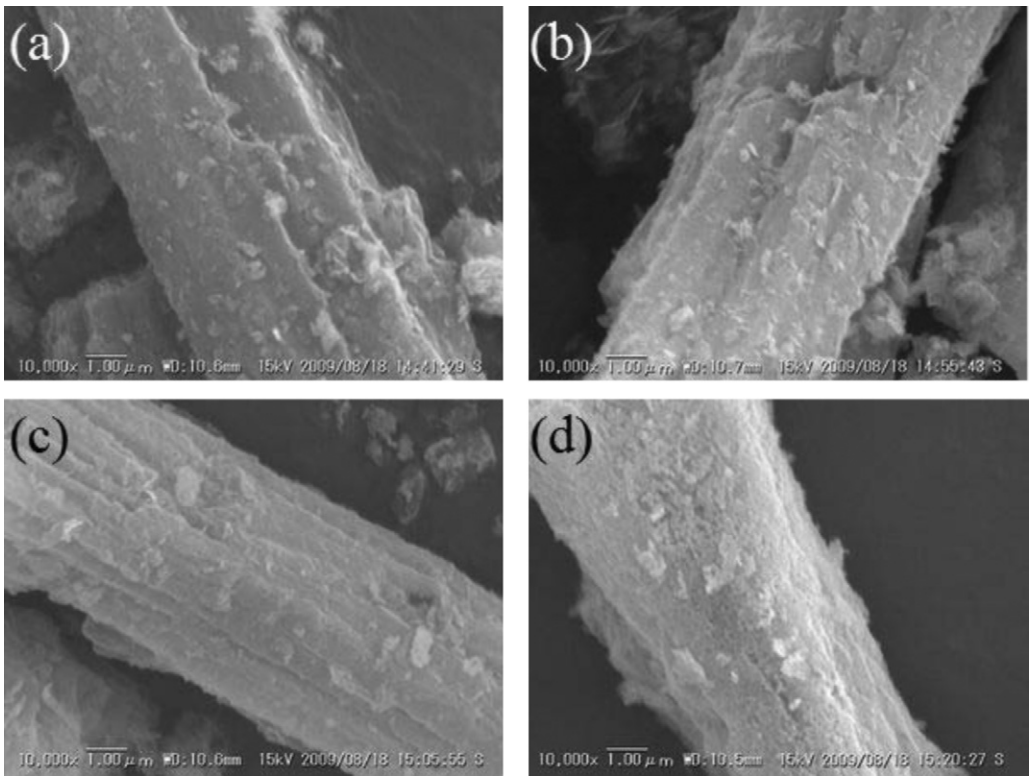

Fig. 2. SEM images of MgO-rich phases obtained by calcination of $MgCO_3$ for 1 h at (a) 873 K, (b) 1073 K, (c) 1273 K, and (d) 1373 K. The scale bars indicate 1 μm.

ferent basicities varied with the calcination temperature. There is a tendency, with increase in the calcination temperature, for the relative intensity of component (*a*) to increase, although it is not clear in which step of the F^- sorption process the basicity and/or base site numbers influence the efficiency of F^- sorption.

The sorption behavior of 9.12 mmol dm^{-3} F^- ions on to the products with different calcination temperatures was observed at 298 K as shown in Fig. 5(a), and the relevant changes of Mg^{2+} concentrations and pH are shown in Fig. 5(b) and (c). The calcination temperature affected the sorption rate and sorption capacity of F^- ions. There is a trend for higher calcination temperature to lead to slower sorption of F^- ions, and the equilibrium concentrations are lower with the higher calcination temperatures except for 873 K-MgO. The anomaly observed with 873-MgO might be caused by the very low crystallinity of MgO and the presence of residual uncalcined impurities of magnesium carbonate (Fig. 1). Ion-exchange with F^- is considered to result from a F^- removal mechanism at the aqueous interface with MgO.

The larger specific surface area of MgO provided much more base sites for ion exchange with anions such as F^- ions at the aqueous interface, leading to the faster initial F^- removal rate, as shown in Fig. 5(a). F^- ions can be exchanged by the formation of an inner-sphere complex on the surface of the metallic oxides [27].

$$\equiv\text{Mg-OH} + F^- \rightleftarrows \equiv\text{Mg-F} + OH^- \quad (1)$$

However, this reaction occurs only at the surface of MgO and affects only the initial F^- removal rate, not the equilibrium.

Release of Mg^{2+} ions was clearly observed in 873 K-MgO (Fig. 5(b)), probably due to the high solubility of the co-existing magnesium carbonates and/or the less crystalline MgO. The maximum released Mg^{2+} concentration was independent of the initial F^- concentration. The released Mg^{2+} ions immediately decreased to reach the equilibrium concentration, and this process was not accompanied by further immobilization of F^- ions on to 873 K-MgO, as shown in Fig. 5(a). In other cases, little release of Mg^{2+} was observed during the sorption process.

The pH increased immediately in all cases (Fig. 5(c)), mainly due to dissolution of MgO, leading to strong alkalization, as shown in

Table 1
Summary of sorbed CO_2 quantities per unit surface area analyzed from CO_2-TPD curves for 1073 K-MgO, 1273 K-MgO and 1373 K-MgO.

	(a)		(b)		(c)		Total CO_2 (mmol m^{-2}) (ratio/%)
	Temperature (K)	CO_2 (mmol m^{-2}) (ratio/%)	Temperature (K)	CO_2 (mmol m^{-2}) (ratio/%)	Temperature (K)	CO_2 (mmol m^{-2}) (ratio/%)	
1073 K-MgO	371	0.0213 (3.12)	424	0.207 (30.44)	553	0.447 (65.72)	0.6753 (100)
1273 K-MgO	371	0.115 (9.19)	424	0.613 (49.22)	553	0.524 (42.04)	1.252 (100)
1373 K-MgO	371	0.189 (12.22)	440	0.527 (34.15)	534	0.842 (54.54)	1.558 (100)

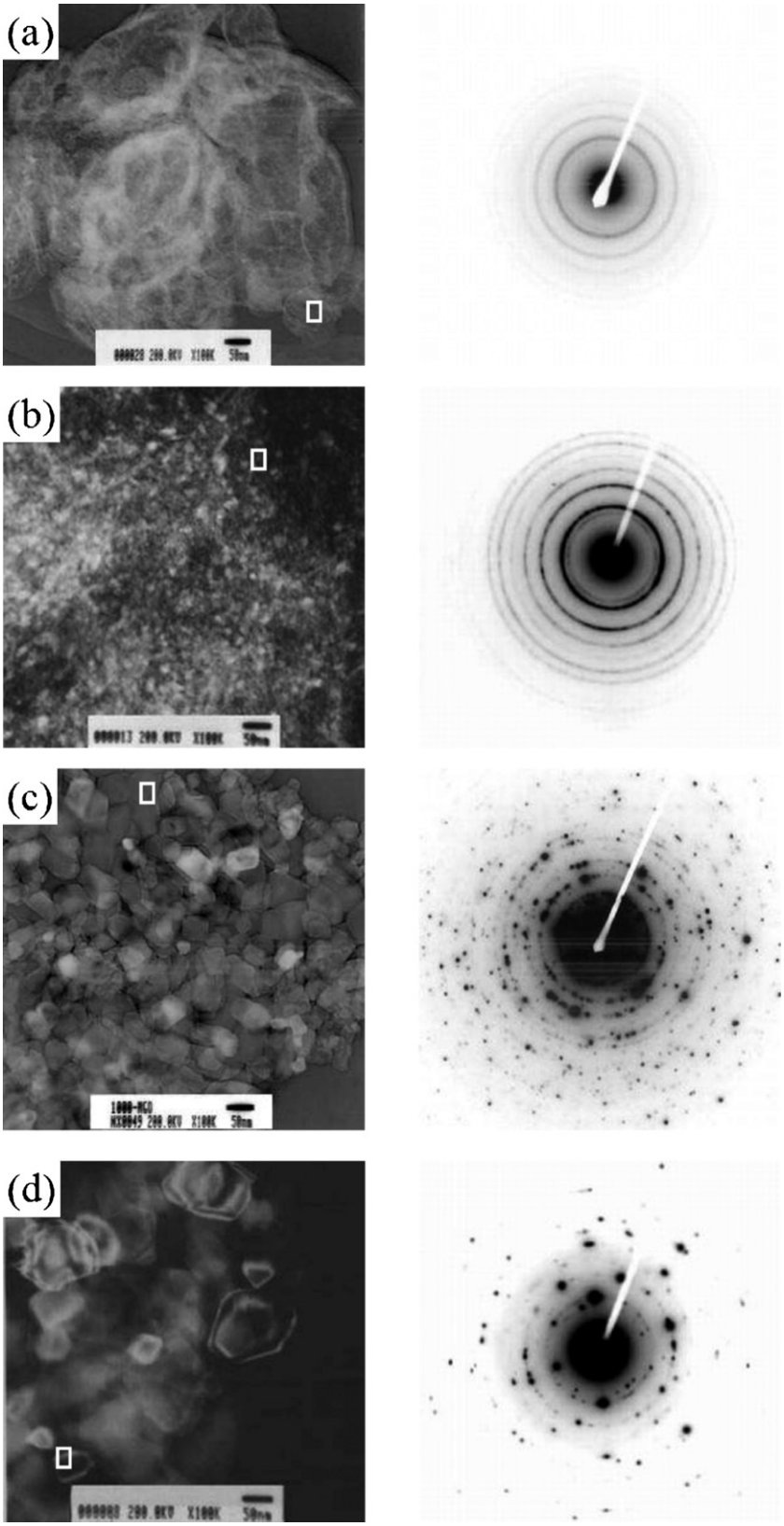

Fig. 3. Bright field TEM images and selected area electron diffraction patterns taken from (a) 873 K-MgO, (b) 1073 K-MgO, (c) 1273 K-MgO and (d) 1373 K-MgO. Horizontal bars in the TEM images indicate 50 nm.

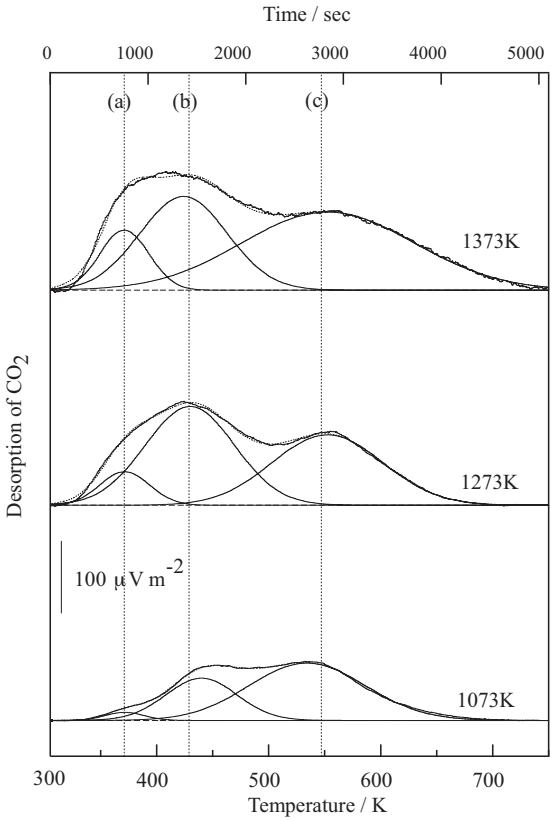

Fig. 4. CO_2-TPD curves and their peak separation for MgO-rich phases prepared with different calcination temperatures.

the following reactions.

$$MgO + H_2O \rightleftarrows Mg^{2+} + 2OH^- \quad (2)$$

$$MgCO_3 \rightleftarrows Mg^{2+} + CO_3^{2-} \quad (3)$$

$$CO_3^{2-} + H_2O \rightleftarrows HCO_3^- + OH^- \quad (4)$$

The equilibrium pH was lower with 1073 K-MgO than 1273 K-MgO and 1373 K-MgO. More crystalline MgO might lead to larger basicity, resulting in the higher reactivity with H_2O [28].

$$\equiv MgO + H_2O \rightleftarrows \equiv Mg\begin{matrix}\delta^+ \\ O_{\delta^-}\end{matrix}\!\!\begin{matrix}O\!:\!H \\ H\end{matrix} \rightleftarrows \equiv Mg\begin{matrix}OH \\ OH\end{matrix} \quad (5)$$

The basicity per unit surface area was the largest with 1373 K-MgO (Table 1). The total surface area is not so important for precipitation, because the initial surface area is immediately affected by coverage with $Mg(OH)_2$ precipitates.

The predominant mechanism in F^- sorption is based on co-precipitation with $Mg(OH)_2$. Therefore, the equilibrium Mg^{2+} concentrations are controlled by the solubility product of $Mg(OH)_2$.

$$Mg^{2+} + 2OH^- \rightleftarrows Mg(OH)_2 \quad K_{sp} 1.1 \times 10^{-11}\,(mol^3/dm^9)\,at\,25\,^\circ C \quad (6)$$

Gulbrandsen et al. [29] reported that F^- enhanced the formation of $Mg(OH)_2$ using electron microscopic investigations. $Mg(OH)_{2-x}F_x$ might also be precipitated when the F^- concentrations are very large [30].

Control experiments were conducted using reagent $MgCO_3$ instead of MgO-rich phases, to understand the sorption of F^- ions on to $MgCO_3$ which is present as impurities in MgO-rich phases of the calcined products at relatively low temperatures. Around 30 mmol dm^{-3} of F^- was removed from 63.36 mmol dm^{-3} of the initial F^- concentration, while only a few mmol dm^{-3} was removed from the solution with the initial F^- concentration at 9.86 mmol dm^{-3}, as shown in Fig. 6(a). In the absence of F^- ions more than 1 mmol dm^{-3} Mg^{2+} ions were released from the $MgCO_3$, while the addition of much more F^- ions suppressed the release of Mg^{2+} ions (Fig. 6(b)). Also, from the result of Fig. 6(b), it can be understood that the release of Mg^{2+} ions is mainly

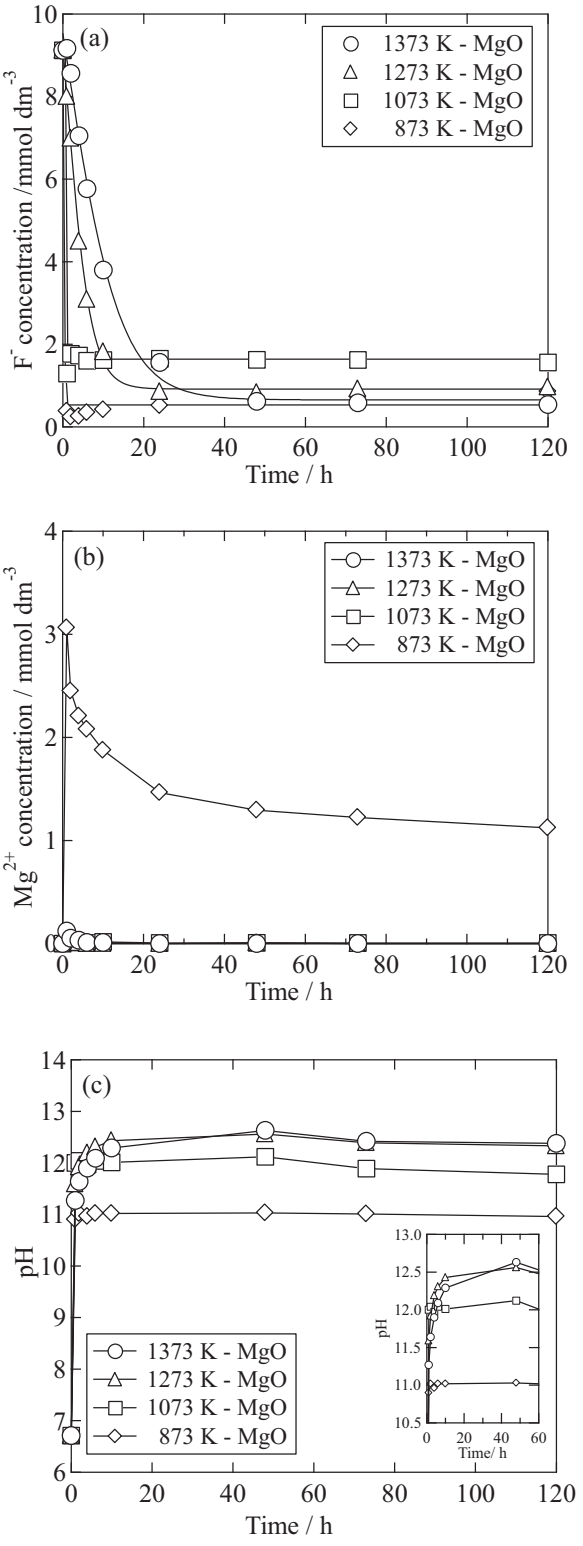

Fig. 5. Changes of (a) F^-, (b) Mg^{2+} concentrations and (c) pH during sorption of F^- at 298 K on MgO-rich phases obtained at different calcination temperatures.

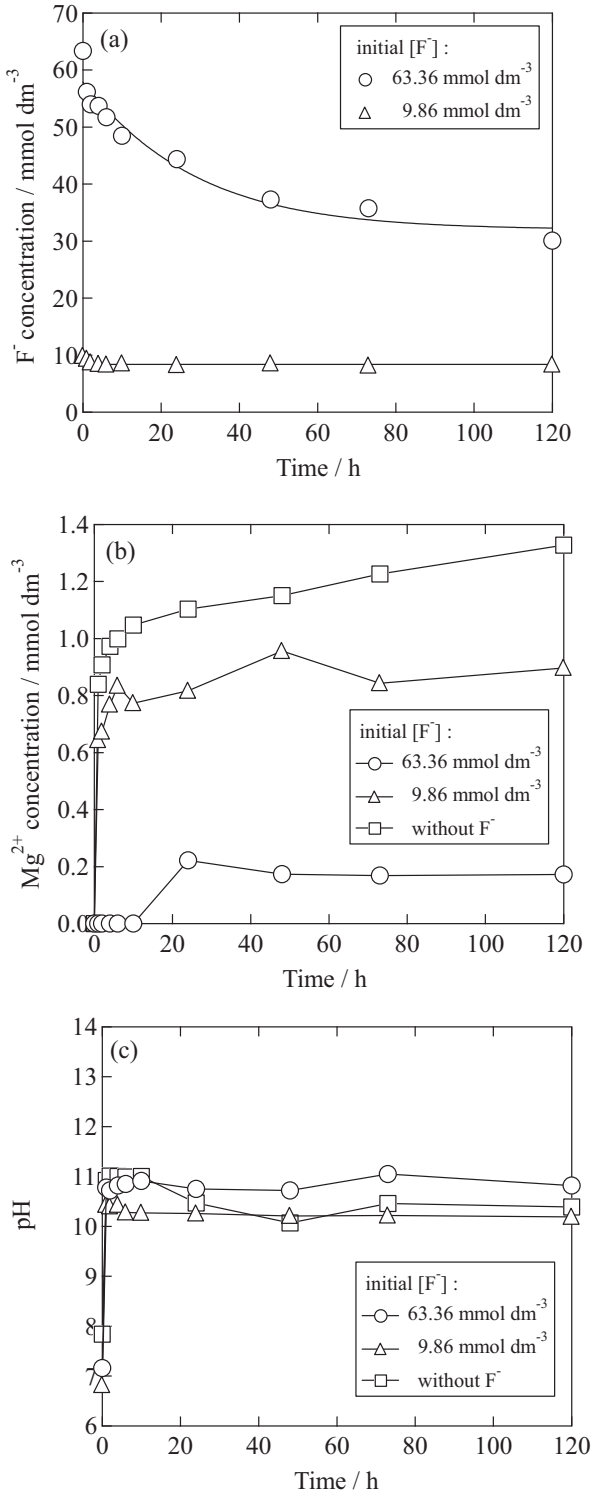

Fig. 6. Changes of (a) F^-, (b) Mg^{2+} concentrations and (c) pH during sorption of F^- at 298 K on basic magnesium carbonate.

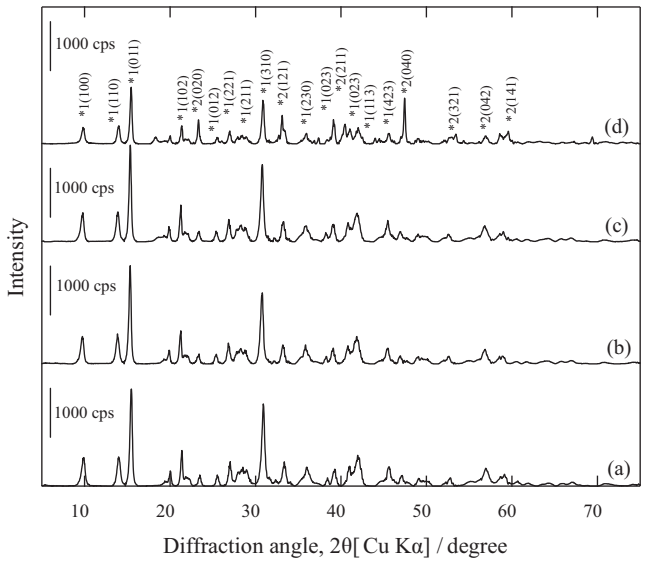

Fig. 7. XRD patterns for (a) basic magnesium carbonate and solid residues after sorption of F^- on basic magnesium carbonate. The initial F^- concentrations are (b) 9.86 mmol dm^{-3}, (c) 63.36 mmol dm^{-3} and (d) zero F^-. The assignment of (*1) is the same as in Fig. 1(a). (*2) $NaMgF_3$ (JCPDS 13-303).

from the less crystalline MgO and only a little from magnesium carbonates in 873 K-MgO, as shown in Fig. 5(b). The equilibrium pH was lower than in the presence of MgO, as shown in Figs. 5(c) and 6(c).

XRD patterns for the solid residues after sorption of F^- ions on the basic magnesium carbonate did not show any significant variation when the initial F^- concentrations are less than 9.86 mmol dm^{-3}, as shown in Fig. 7. Above this concentration, the basic magnesium carbonates remain and an additional phase $NaMgF_3$ was observed (JCPDS 13-303) in the solid residues after sorption of 63.36 mmol dm^{-3} F^- ions [29]. The saturation index of MgF_2 was calculated to be 3.99 and 4.39 at equilibrium for 9.86 mmol dm^{-3} and 63.36 mmol dm^{-3} initial F^- concentrations, respectively. However, MgF_2 precipitates were not observed in Fig. 7(c) and (d), and $NaMgF_3$ was observed in Fig. 7(d). This suggests that the solid solution of $NaMgF_3$ might be more stabilized over MgF_2 and NaF in the presence of high F^- concentrations.

The sorption isotherm of F^- ions on the calcined products of the MgO-rich phases at different temperatures is summarized in Fig. 8, in which C_e and Q are defined as the equilibrium concentration (mmol dm^{-3}) and the sorbed quantity of F^- ions on unit weight of sorbents (mmol g^{-1}). In this figure, the two points obtained using basic magnesium carbonate were added to compare with the calcined, MgO-rich phases. Apparently 873 K-MgO has the largest capacity for F^- sorption, as shown in Fig. 8(a). As shown in Fig. 1, 873 K-MgO includes basic magnesium carbonates which contribute to the removal of F^- by co-precipitation with other types of basic carbonate and less crystalline MgO with high solubility, to influence the destructive sorption of F^-. Therefore, the trend of the sorption isotherm with 873 K-MgO is quite exceptional and different from the others. However, when focusing on the details of the region of the isotherm below 2.0 mmol dm^{-3} of C_e, as shown in Fig. 8(b), greater sorption capacities were obtained with the original sorbents calcined at higher temperatures for the range less than 9.12 mmol dm^{-3} of the initial F^- concentration, except for 873 K-MgO. This trend can be explained by neither the solubility nor the specific surface area of the MgO-rich phases.

The range of F^- concentrations in Fig. 8(b) is often used and is of practical importance in the treatment of industrial discharges impacted by F^- ions. When 1073 K-MgO is used to remove F^- from an initial concentration of 9.12 mmol dm^{-3} the equilibrium concentration is 1.6 mmol dm^{-3} (30.4 mg/L), which corresponds to three times the MCL value. However, when 1373 K-MgO is applied to remove F^- from the same initial concentration, the equilibrium

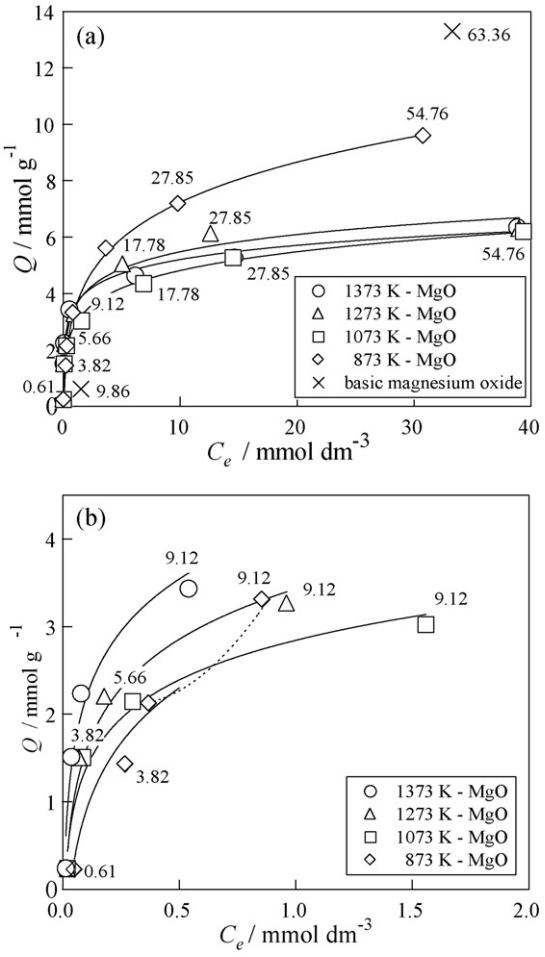

Fig. 8. Sorption isotherms of F^- on MgO-rich phases at different calcination temperatures. The region below $C_e = 0.8$ mmol dm^{-3} in (a) is expanded, as shown in (b). The numbers (mmol dm^{-3}) in both figures indicate the initial F^- concentrations.

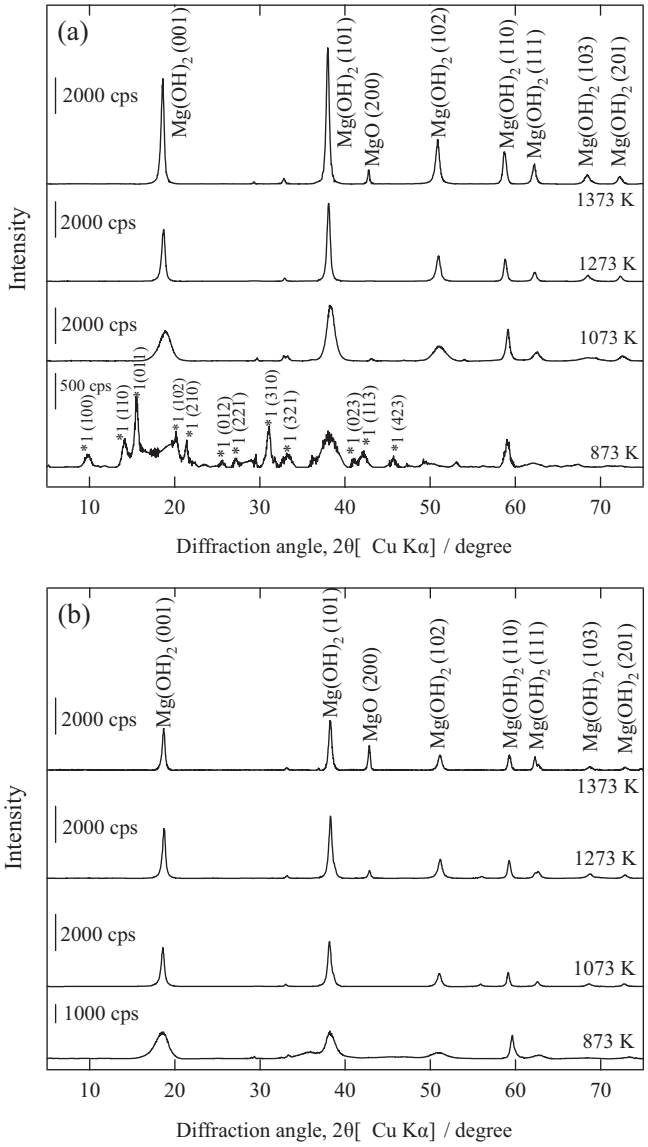

Fig. 9. XRD patterns of solid residues after sorption of F^- using MgO-rich phases obtained by calcination at different temperatures. The initial F^- concentrations are (a) 9.12 mmol dm^{-3} and (b) 54.76 mmol dm^{-3}. (*1) $Mg_5(CO_3)_4(OH)_2{\cdot}4H_2O$ (JCPDS 25-513).

concentration is close to the MCL value. This means that there is a region of F^- concentrations where the total basicity per unit surface area might be a more important affect than the specific surface area to the initial step of sorption of F^- ions on to the MgO-rich phases.

The XRD patterns of solid residues after sorption of F^- using the MgO-rich phases obtained by calcination at different temperatures are shown in Fig. 9(a) and (b) for 9.12 mmol dm^{-3} and 54.76 mmol dm^{-3} of initial F^- concentrations, respectively. There are major peaks assigned to $Mg(OH)_2$ (JCPDS 44-1482), one clear peak at 42.8° 2θ assigned to MgO (JCPDS 45-946) for the calcinations temperature 1373 K and some minor peaks assigned to $Mg_5(CO_3)_4(OH)_2{\cdot}4H_2O$ (JCPDS 25-513) for the 873 K calcination temperature, as shown in Fig. 9(a). There is a tendency for lower calcination temperature to produce MgO-rich phases with less crystalline $Mg(OH)_2$ after sorption of F^- ions. The initial sorbent crystallinity of MgO is strongly affected by the crystallinity of $Mg(OH)_2$, which is the solid residue after sorption of F^-, suggesting that the crystal seeds of $Mg(OH)_2$ might be formed in the vicinity of the surface of MgO, as shown in Eq. (5). The crystallinity of MgO also influenced the equilibrium F^- concentrations, as shown in Fig. 8(b).

When the initial F^- concentration is 54.76 mmol dm^{-3}, the Q value for 873 K-MgO was 1.7 times larger that those for the others (Fig. 8(a)). The broadening was clearly observed in the solid residue for 873 K-MgO (Fig. 8(b)) because of the crystal strain of $Mg(OH)_2$ produced by inclusion of many more F^- ions or perhaps the formation of $Mg(OH)_{2-x}F_x$. Much larger concentrations of F^- ions stabilized the formation of $Mg(OH)_2$ rather than the basic magnesium carbonates [29].

Fig. 10 shows SEM images for the same samples whose XRD is given in Fig. 9. These images show the morphological changes from the calcined products before sorption of F^- ions in Fig. 2. There are submicron-sized honeycomb structures with solid residues for 873-MgO and 1073-MgO, as shown in Fig. 10(a), (b), (e) and (f) Fig. 10. Phases other than $Mg(OH)_2$ in 873-MgO (Fig. 9(a)) were not clearly reflected in the SEM image (Fig. 10(a)). In the cases of 1273-MgO and 1373-MgO, the surfaces of the solid residues after sorption were covered with very fine flakes, probably showing that the development of $Mg(OH)_2$ precipitates became obvious in Fig. 10(c), (g) and especially in Fig. 10(d) and (h) because of the large F^- concentration. The interpretation is mostly consistent with the XRD results (Fig. 9).

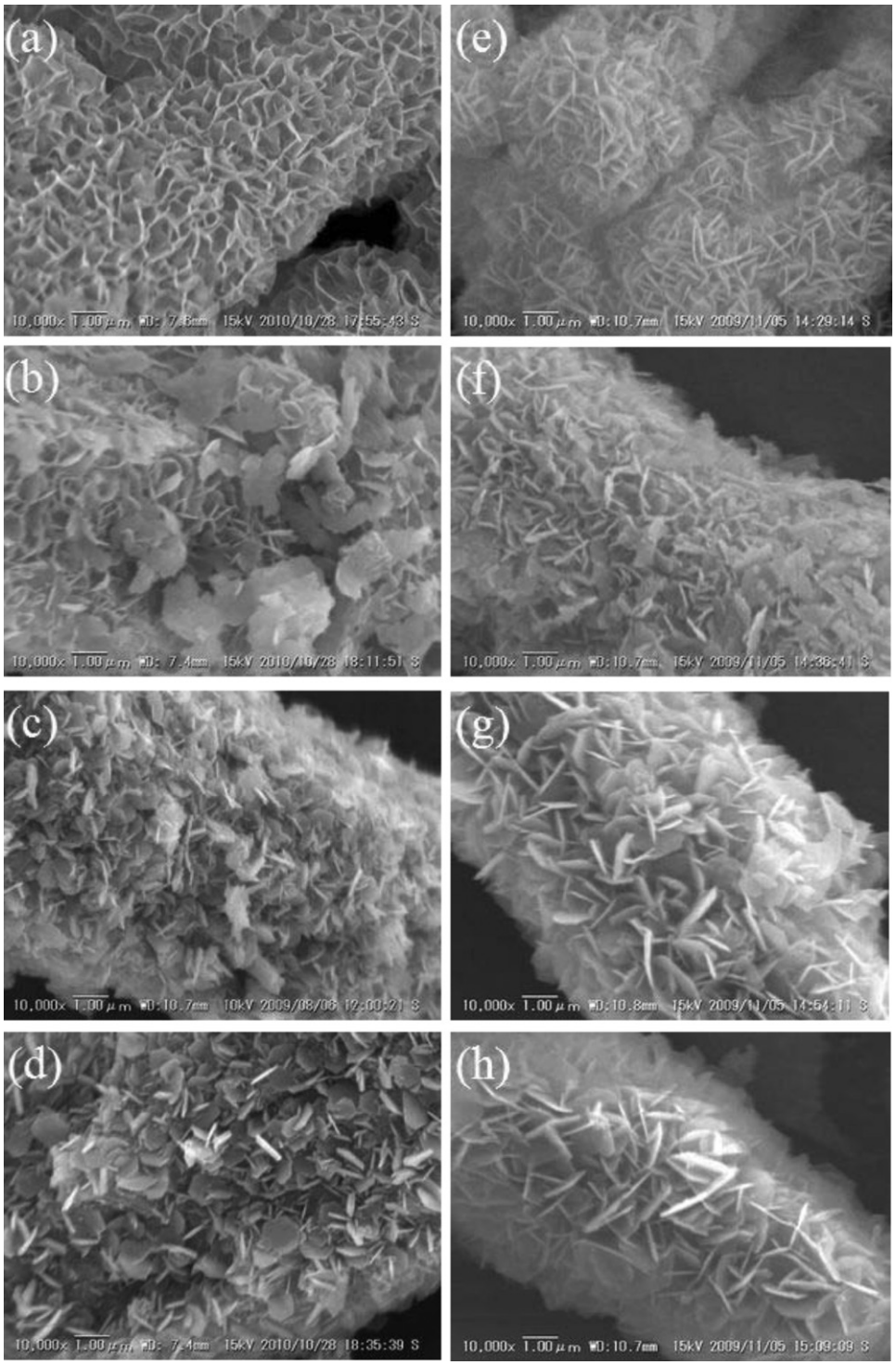

Fig. 10. SEM images of MgO-rich phases after sorption of (a)–(d) 9.12 mmol dm^{-3} and (e)–(h) 54.76 mmol dm^{-3} F^- ions. The scale bars indicate 1 μm. (a) and (e) 873 K-MgO, (b) and (f) 1073 K-MgO, (c) and (g) 1273 K-MgO and (d) and (h) 1373 K-MgO.

4. Conclusions

The effect of calcination temperature during production of magnesium oxides on the sorption of F^- ions has been investigated. Characterization of calcined MgO-rich phases at different temperatures by XRD, TEM, and electron diffraction has revealed that the higher calcination temperatures produced more crystalline and larger MgO crystals. The CO_2-TPD analysis, which provides the information about basicity and quantities of base sites, indicated that higher calcination temperatures produced higher basicity per unit surface area.

In a range around MCL for the F^- concentration, the calcination temperature affected the sorption density of F^- ions on magnesium oxides. Higher calcination temperatures caused greater sorption of F^- ions. In contrast, in a range of $C_e > 0.5$ mmol dm^{-3} the destructive sorption of F^- on to less crystalline MgO with lower calcinations temperature becomes predominant, leading to greater F^- sorption.

These results suggest that the calcination temperature used to produce MgO strongly affects the efficiency and longevity of permeable reactive barriers, including MgO, used to treat F^- ions in groundwaters, depending on the F^- concentration.

Acknowledgements

Financial support was provided to KS by Japan Society for Promotion of Science (JSPS) Grant in Aid for Scientific Research No. 22246117, Funding Program for Next Generation of World-Leading Researchers (GR078), and Japan Science and Technology Agency (JST). The collection of XRD patterns was performed at the Center of Advanced Instrumental Analysis, and TEM images were collected at the Research Laboratory for High Voltage Electron Microscopy (HVEM) in Kyushu University. The CO_2-TPD curves were obtained by courtesy of Prof. Yasutake Teraoka at Department of Energy and Material Sciences, Kyushu University.

References

[1] M.D. Herta Spencer, M.D. Isaac Lewin, B.S. Emilie Wistrowski1, Ph.D. Joseph Samachson, Fluoride metabolism in man, Am. J. Med. 49 (6) (1970) 807–881.
[2] R.C. Meenakshi, Maheshwari, Fluoride in drinking water and its removal, J. Hazard. Mater. B137 (2006) 456–463.
[3] O. Oren, Y. Yechieli, J.K. Bohlke, A. Dody, Contamination of groundwater under cultivated fields in an arid environment, Central Arava Valley, Israel, J. Hydrol. 290 (3/4) (2004) 312–328.
[4] F. Anwar, Assessment and analysis of industrial liquid waste and sludge disposal at unlined landfill sites in arid climate, Waste Manage. 23 (9) (2003) 817–824.
[5] M.C. Bell, T.G. Ludwig, The supply of fluoride to man: ingestion from water, in: Fluorides Human Health W.H.O. Monograph Series 59, World Health Organization, Geneva, 1970.
[6] The Japan Society Analytical Chemistry, Hokkaido Branch, Mizu No Bunseki, Kagakudojin. 5, 2005, pp. 28–29.
[7] M.M. Scherer, S. Richter, R.L. Valentine, P.J.J. Alvarez, Chemistry and microbiology of permeable reactive barriers for in situ groundwater clean up, Crit. Rev. Environ. Sci. Technol. 30 (2000) 363–411.
[8] D.L. Naftz, S.J. Morrison, J.A. Davis, C.C. Fuller, Handbook of Groundwater Remediation Using Permeable Reactive Barriers: Applications to Radionuclides, Trace Metals, and Nutrients, Academic Press, San Diego, CA, 2003, pp. 1–5.
[9] K. Sasaki, H. Takamori, S. Moriyama, H. Yoshizaka, T. Hirajima, Effect of saw dust on borate removal from groundwater in bench-scale simulation of permeable reactive barriers including magnesium oxide, J. Hazard. Mater. 185 (2011) 1440–1447.
[10] P.L. Bishop, G. Sansoucy, Fluoride removal from drinking water by fluidized activated alumina adsorption, J. AWWA 70 (1978) 554–559.
[11] K. Muthukumaran, N. Balasubramanian, T.V. Ramakrishna, Removal of fluoride by chemically activated carbon, Ind. J. Environ. Protect. 15 (7) (1995) 514–517.
[12] W. Rongshu, H. Li, P. Na, W. Ying, Study of a new adsorbent for fluoride removal from waters, Water Qual. Res. J. Can. 30 (1) (1995) 81–88.
[13] T. Kameda, N. Uchiyama, K.S. Park, G. Grause, T. Yoshioka, Removal of hydrogen chloride from gaseous streams using magnesium–aluminum oxide, Chemosphere 73 (2008) 844–847.
[14] G. Wu, X. Wang, W. Wei, Y. Sun, Fluorine-modified Mg–Al mixed oxides: a solid base with variable basic sites and tunable basicity, Appl. Catal. A: Gen. 377 (2010) 107–113.
[15] C.D. Nava, M.S. Rios, M.T. Olguin, Sorption of fluoride ions from aqueous solutions and well drinking water by thermally heated hydrocalcite, Sep. Sci. Technol. 38 (1) (2003) 131–147.
[16] D.P. Das, J. Das, K. Parida, Physicochemical characterization and adsorption behavior of calcined Zn/Al hydrotalcite-like compound (HTlc) towards removal of fluoride from aqueous solution, J. Colloid Interface Sci. 261 (2003) 213–220.
[17] H. Wang, J. Chen, Y. Cai, J. Ji, L. Liu, H.H. Teng, Defluoridation of drinking water by Mg/Al hydrotalcite-like compounds and their calcined products, Appl. Clay Sci. 35 (2007) 59–66.
[18] L. Lv, J. Hea, M. Wei, D.G. Evans, X. Duan, Factors influencing the removal of fluoride from aqueous solution by calcined Mg–Al–CO_3 layered double hydroxides, J. Hazard. Mater. B133 (2006) 119–128.
[19] W. Nigussie, F. Zewgeb, B.S. Chandravanshi, Removal of excess fluoride from water using waste residue from alum manufacturing process, J. Hazard. Mater. 147 (2007) 954–963.
[20] A.K. Yadav, C.P. Kaushik, A.K. Haritash, A. Kansal, N. Rani, Defluoridation of groundwater using brick powder as an adsorbent, J. Hazard. Mater. B128 (2006) 289–293.
[21] S. Kagne, S. Jagtap, P. Dhawade, S.P. Kamble, S. Devotta, S.S. Rayalu, Hydrated cement: a promising adsorbent for the removal of fluoride from aqueous solution, J. Hazard. Mater. 154 (2008) 88–95.
[22] M.G. Sujana, H.K. Pradhan, S. Anand, Studies on sorption of some geomaterials for fluoride removal from aqueous solutions, J. Hazard. Mater. 161 (2009) 120–125.
[23] J. Zhang, S. Xie, Y.S. Ho, Removal of fluoride ions from aqueous solution using modified attapulgite as adsorbent, J. Hazard. Mater. 165 (2009) 218–222.
[24] H. Hattori, Solid base catalysts: generation, characterization, and catalytic behaviour of basic sites, J. Japan Petroleum Inst. 47 (2) (2004) 67–81.
[25] T. Ito, J. Isawa, H. Kishimoto, H. Kobayashi, K. Toi, Nature of CO_2 adsorbed on MgO surface at low temperature, in: T. Inui, M. Anpo, K. Izui, S. Yanagida, T. Yamaguchi (Eds.), Advances in Chemical Conversations for Mitigating Carbon Dioxide, Studies in Surface Science and Catalysis, vol. 114, 1998, 391-394.
[26] S. Fan, N. Zhao, J. Li, F. Xiao, W. Wei, Y. Sun, Effective and green synthesis of methyl pyrrole-1-carboxylate with dimethyl carbonate over solid base, Catal. Lett. 120 (2008) 299–302.
[27] W. Stumm, J.J. Morgan, Aquatic Chemistry, 3rd ed., Wiley-Interscience Publication, New York, USA, 1996, p. 541.
[28] J.L. Anchell, A.C. Hess, H_2O dissociation at low-coordinated sites on $(MgO)_n$ Clusters, $n = 4$, 8, J. Phys. Chem. 100 (1996) 18317–18321.
[29] E. Gulbrandsen, J. Tafto, A. Olsen, The passivation of Mg in alkaline fluoride solutions. Electrochemical and electron microscopical investigations, Corros. Sci. 34 (9) (1993) 1423–1440.
[30] P.M. Bradford, B. Case, G. Dear-Aley, J.F. Turner, I.S. Woolsey, Ion beam analysis of corrosion films on a high magnesium alloy (MAGNOX AL 80), Corros. Sci. 16 (1976) 747–766.